Handbook of Research on Hydroinformatics:

Technologies, Theories and Applications

Tagelsir Mohamed Gasmelseid
King Faisal University, Saudi Arabia

Information Science REFERENCE

INFORMATION SCIENCE REFERENCE

Hershey · New York

Director of Editorial Content: Kristin Klinger
Director of Book Publications: Julia Mosemann
Acquisitions Editor: Lindsay Johnston
Development Editor: Joel Gamon
Publishing Assistant: Casey Conapitski
Typesetter: Deanna Jo Zombro
Production Editor: Jamie Snavely
Cover Design: Lisa Tosheff

Published in the United States of America by
Information Science Reference (an imprint of IGI Global)
701 E. Chocolate Avenue
Hershey PA 17033
Tel: 717-533-8845
Fax: 717-533-8661
E-mail: cust@igi-global.com
Web site: http://www.igi-global.com

Library of Congress Cataloging-in-Publication Data

Handbook of research on hydroinformatics : technologies, theories and applications / Tagelsir Mohamed Gasmelseid, editor.
p. cm.
Includes bibliographical references and index.
Summary: "This book provides relevant theoretical frameworks and empirical research findings in the area hydroinformatics to assist professionals to improve their understanding of the development and use of decision support tools to support decision making and integrated water management at different organizational levels and domains"--Provided by publisher. ISBN 978-1-61520-907-1 (hardcover) -- ISBN 978-1-61520-908-8 (ebook) 1. Hydrology--Data processing. 2. Hydrologic models I. Gasmelseid, Tagelsir Mohamed, 1967- GB656.2.E53H36 2010
551.480285--dc22
2010000961

British Cataloguing in Publication Data
A Cataloguing in Publication record for this book is available from the British Library.

Chapter 12
Integrated Flood Risk Analysis for Assessing Flood Protection Strategies

J. Ernst
University of Liège, Belgium

B.J. Dewals
Fund for Scientific Research F.R.S.-FNRS, Belgium

S. Detrembleur
University of Liège, Belgium

P. Archambeau
University of Liège, Belgium

S. Erpicum
University of Liège, Belgium

M. Pirotton
University of Liège, Belgium

ABSTRACT

The present chapter describes an end-to-end methodology for assessing flood protection strategies, including the whole methodological process from hydrological statistics to detailed 2D hydraulic modelling, damage calculation and flood risk evaluation. This risk-based approach serves as a component of a decision-support system (DSS) developed in Belgium for identifying cost-effective flood management strategies in the context of climate change. The DSS accounts for both hydraulic and socio-economic parameters to quantify the benefits (in terms of avoided risk) and the cost of each strategy. Besides reviewing fundamentals of flood risk assessment, including the inundation model and main concepts related to flood risk, a consistent methodology for micro-scale flood risk analysis is presented in detail, combining complementary sources of GIS information such as high resolution and high accuracy land use database as well as socio-economic datasets. Finally a case study on a main tributary of river Meuse in Belgium is described.

DOI: 10.4018/978-1-61520-907-1.ch012

INTRODUCTION

For centuries people have settled in areas nearby rivers. They exploited rivers for many purposes, such as inland navigation, fishery, irrigation in dry regions or electricity production. They also had to face inundation events but, to a certain extent, they adapted their settlements and their behaviour to cope with this hazard. Flood occurrence and the consequences of flooding were generally accepted by society.

Nowadays, riversides are becoming more and more urbanized but the communities living along rivers tend not to accept the risk of flooding any longer. Drastic reductions in flood risk are requested. Moreover, within the framework of climate change, heavy precipitations are expected to increase in terms of frequency and intensity (IPCC 2001). In this context, it is reasonable to think that peak discharges in rivers will also rise and such events will become more frequent. Thus, protection of people threatened by flooding and integrated flood risk management are becoming issues of growing importance.

At present, the design and the optimization of flood protections is gradually shifting from a method based on a single return period to a full risk analysis, which takes into account a large range of occurrence probability (Merz 2006). This type of approach may lead to cost benefit analyses, for which predicted losses are estimated from the risk analysis procedure. This chapter is in line with the framework of this emerging approach for elaborating flood management strategies. Indeed, the procedure detailed in this chapter relies on a risk modelling chain handling the data flow from statistical analysis of river flows to the risk evaluation. This risk modelling system enables to assess psycho-social impacts of floods as well as direct and tangible economic losses, with the aim of designing and optimising local flood protection strategies.

While most risk analyses are performed at macro- or meso-scale, in this chapter an original micro-scale analysis is described. It means that each asset (house, company, public building …) is analyzed individually. Such a refined investigation leads to detailed economic as well as psycho-social damage evaluations which prove to be helpful to rank different adaptation measures (e.g. mobile dikes, rehabilitation of floodplains, diversion channel …) in terms of overall effectiveness.

The developed tool also handles a large number of detailed and accurate input data necessary in such a micro-scale analysis. First, 2D flow modelling is essential for providing as an output high resolution flood maps detailing the distribution of water depth and flow velocity in the floodplains and representing interactions between main channel and floodplains. Secondly, accurate land use databases have to be used in order to identify each building individually and for determining their type (residential, industrial, petrol station …).

RISK ANALYSIS METHODOLOGY

Fundamentals

Flood risk is generally defined as the product of *hazard* and *vulnerability* (Apel *et al.* 2007). The hazard component of risk is related to the statistical and the physical characteristics of the considered floods. The occurrence or exceedance probability of a flood is typically derived from its statistical return period commonly used in hydrological sciences. The vulnerability results from a combination of the *exposure* of the elements-at-risk, such as number of threatened people and other affected assets, with their *susceptibility*.

This view of the concept of risk is consistent with Directive 2007/60/EC of the European Union, which states: "flood risk means the combination of the probability of a flood event and the potential adverse consequences for human health, the environment, cultural heritage and economic activity associated with a flood event" (EU 2007). As shown in Figure 1, the evaluation

Figure 1. Main components of flood risk (Dewals et al. 2008c; Ernst et al. 2008)

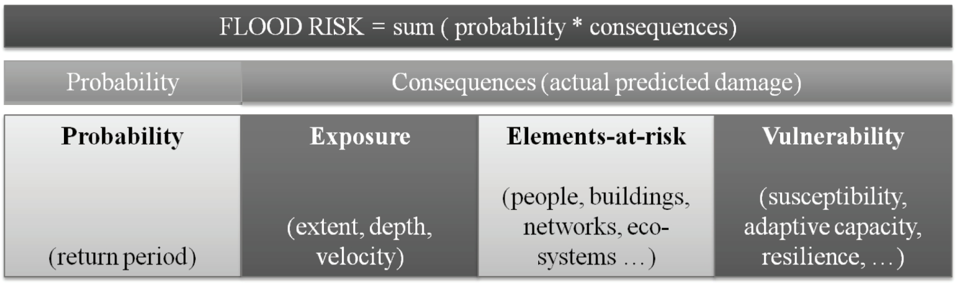

of the risk from flooding relies basically on two main parameters: the *probability of occurrence* of each flood event and its *consequences*, expressed as the induced damages.

The four main parameters of flood risk, namely, probability, exposure, element-at-risk and vulnerability may be defined as follows:

- In hydrology and river management, the probability associated to a given flood is typically expressed as a return period in years (e.g. the discharge value of a 20-year return period flood would statistically be exceeded once in a period of 20 years).
- The exposure is the set of values of the hydraulic parameters of a flood event affecting the assets and the people in the floodplains. Hydraulic parameters typically include the inundation extent, the water depth and the flow velocity, the rising rate of water and the duration of the flood. This information is directly derived from numerical flow modelling.
- The elements-at-risk are people, dwellings, industrial buildings, road and rail network as well as others facilities which may be affected by a flood event.
- Their vulnerability results from the combination of several parameters such as resilience, i.e. capacity of an element to recover its initial state, and susceptibility, i.e. the propensity of a particular receptor to experience harm.

Methodology

Flood risk may be practically evaluated following the process described in the flow chart of Figure 2, which also shows the main input data needed as well as the outcomes of the methodology.

The procedure involves the following four basic steps:

1. first, statistical analysis of hydrological data provides the exceedance probability of each considered flood discharge and, if relevant, this may be complemented by assumptions regarding impacts of future climate change on the river hydrology;
2. next, hydraulic modelling is conducted to generate hazard maps (i.e. inundation extent, water depth and velocity field corresponding to each exceedance probability);
3. by combining the predicted inundation extent and geographical data such as land use and location of buildings, the exposure may be evaluated;
4. finally, the flood impacts may be computed by conducting socio-economic analyses, based on social indexes and economic damage functions, which lead eventually to the risk evaluation.

While step 1 is considered as input data in the present study, the application of the rest of this four-step procedure is described in detail in the next paragraphs.

Figure 2. Flow chart describing the risk analysis procedure along with main input and outcomes

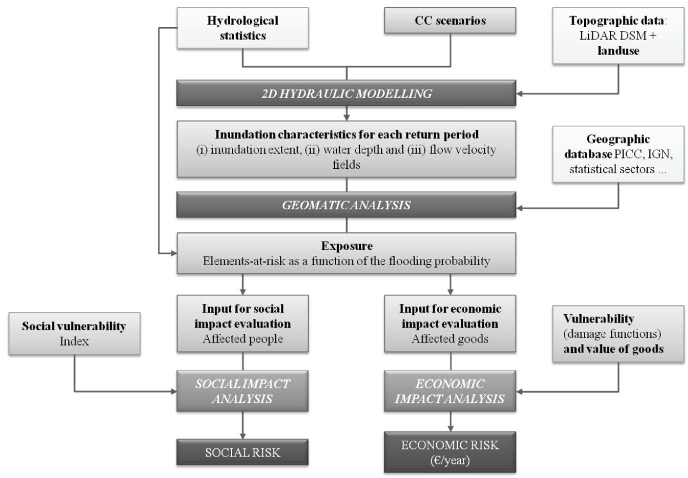

Hydraulic Flood Mapping: Hazard

The hydrological study of the catchment response and the river flow time series provides the inflow boundary conditions to be prescribed for hydraulic modelling. Possible climate change impacts may be taken into account at this stage by adapting the hydraulic boundary conditions or their associated exceedance probability.

Consistency between the analysis scales for inundation mapping and for the rest of the risk analysis is important. Thus, in accordance with the micro-scale approach followed here, flow computations must enable to predict water depth and flow velocity at the scale of individual buildings in all floodplains.

For this purpose, simplified 1D flow models, such as often used as hydrodynamic input data for flood loss estimation, are basically unable to reach a satisfactory accuracy. Moreover, for damage quantification in particular in strongly urbanized areas, one dimensional flow models have already been reported to provide too coarse approximations of the flow field (McMillan and Brasington 2008). Therefore, fully dynamic two-dimensional flow modelling is used here, with the aim of modelling properly the interactions between the main riverbed and the floodplains, as well as to account for the complex topographic structures of urbanized floodplains.

Geomatic: Exposure

The third step consists in combining the flood maps and the land use databases in order to identify the affected assets.

Since water depth is the main parameter influencing damages, this value needs to be known for each individual element-at-risk. However, since hydraulic modelling is run on a Digital Surface Model, which includes obstacles relevant to the flow such as buildings, the water level inside these over grounded structures cannot be deduced directly from the modelling results (since computed water depths are zero at the location of buildings). Therefore, two techniques have been implemented to evaluate the water depth inside buildings:

- either the average of the water depth computed in the wet cells connected to the considered asset is used (Figure 3 a.),
- or the ground level and the free surface elevation in the vicinity of the asset are linearly interpolated based on a least square method and the water depth inside the

Figure 3. Sketch of both techniques used to evaluate the water depth inside over grounded assets

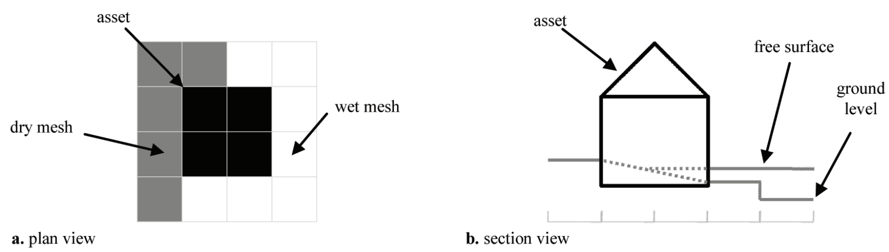

building is deduced from this interpolation (Figure 3 b.).

As a result, a value of water depth may be ascribed to each asset.

Figure 4 shows an example of output of the exposure analysis. In this example, the houses affected by the inundation are classified as a function of the water depth, based on a standard three-class ranking commonly used for inundation mapping in Belgium: inundation depth *(i)* below 0.3 meter, *(ii)* between 0.3 and 1.3 meter and *(iii)* above 1.3 meter.

Socio-Economic Risk

The fourth step of the risk evaluation procedure is the impact analysis, which leads to the socio-economic risk assessment.

Psycho Social Impact

The social flood impact is a function of three main parameters. First, the *flood characteristics*: the social impact depends on the water level, the water rising rate, the flow velocity and the duration of flooding. Second, the *vulnerability* of the people-at-risk: some population groups may have more difficulties in coping with flooding than others. Third, the *adaptive capacity* of communities, i.e. the capacity available in the society to adapt to floods: measures existing to support people during and after flooding.

The social vulnerability and the adaptive capacity of people is evaluated by means of a composed index that incorporates socio-economic data, such as age, health condition, financial status, property type, nationality and family composition at the district level (Coninx & Bachus 2007). The

Figure 4. Example of result of exposure analysis: number of inundated houses as a function of the discharge (black curves: all houses, grey curves: water depth ≤ 1.3m, light grey curves: water depth ≤ 0.3m)

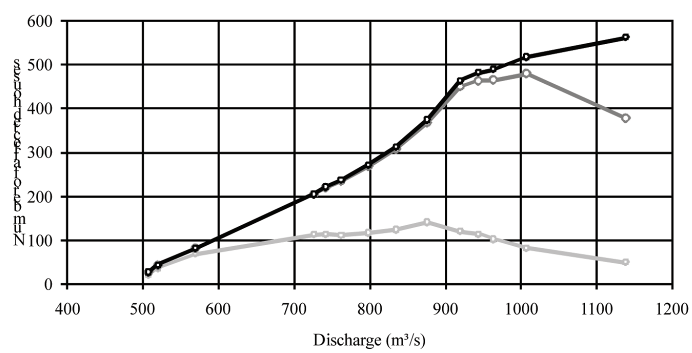

social impact is computed as a combination of these social vulnerability and adaptive capacity indices and the flood characteristics, leading to a flood impact index enabling to distinguish between three social impact categories: *(i)* low, *(ii)* medium or *(iii)* high.

In the next graph (Figure 5), the psycho-social vulnerability results are plotted as a function of the exceedance probability (Ernst *et al.* 2009a; Ernst *et al.* 2009b). Note that there are no people affected by high social impact in this example. The graph in Figure 5 is called *risk curve* (Kaplan & Garrick 1981) and constitutes a genuine expression of the risk since it links the impact (or damage) to the corresponding exceedance probability. To avoid significant losses of information, Kaplan and Garric (1981) advise not to reduce such curves to a single risk value or indicator, since "*a single number is not a big enough concept to communicate risk*".

Economic Impact

The economic impact analysis is based on stage-damage curves or damage functions, linking the hydraulic parameters, typically only the water depth and the expected damage encountered by the elements-at-risk. Such depth damage functions are internationally accepted as a standard approach to assess flood damage (Smith 1994). Two main types of damage functions are available:

- absolute depth-damage functions, which relate the damage to water depth,
- and relative depth-damage functions, which lead to an estimation of a loss ratio compared to the total value of the affected asset.

The later kind of damage functions is predominantly used (Merz *et al.* 2004), because of the possibility to apply these functions in different regions and countries without changing the damage estimation model itself, but simply by adapting the estimation of the asset value. In this study, the recently developed Flood Loss Estimation Model - FLEMO was used because it was developed to be applicable to micro-scale risk analysis (Thieken *et al.* 2008).

The economic impact evaluation consists in combining the computed water depth inside the elements-at-risk and the depth-damage functions (Ernst *et al.* 2008). Typical results are plotted in the graph of Figure 6.

Since the present methodology is applied mainly to urbanized areas with limited areas of

Figure 5. Example of output of the risk modelling process in terms of social impact as a function of the exceedance probability

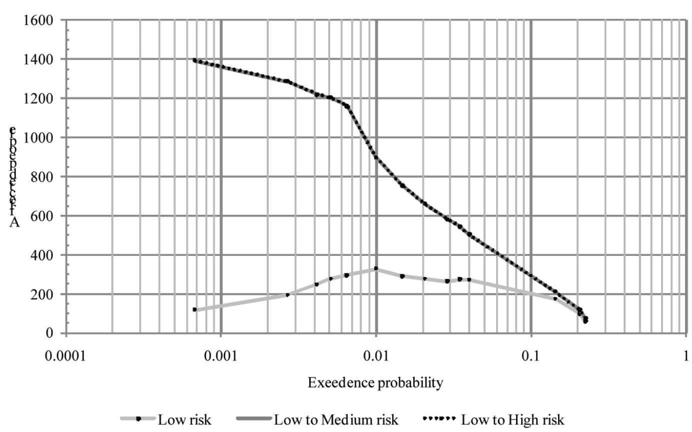

Figure 6. Example of output of the risk modelling process in terms of damage compared to the damage corresponding to a 100 year flood, as a function of flow rate (may be alternatively expressed as a function of return period or exceedance probability)

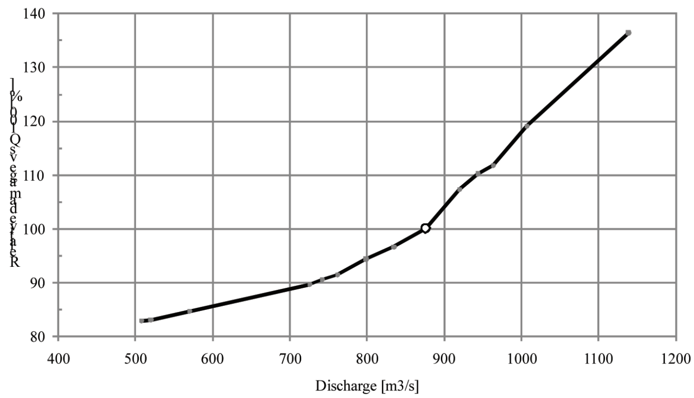

Simulated values of the labelled trends:

1: Projected Lake Volume (from 2750 to 2752 km^3)
2: Nile outflow (from 33.63 to 34.04 km^3/year)
3: Jinja gauge level (from 11.93 to 11.96 m)
4: Water withdrawal by riparian population over the years not considered (population growth not factored into this model)

crops or fields, this chapter focuses on socio-economic impacts of floods on household and people, whereas environmental and agronomic issues such as soil erosion or effects on vegetation and animals were disregarded.

HYDRAULIC MODEL

As an onset for evaluating socio-economic impacts of floods, simulations of floodplain inundation flows are conducted with the numerical model WOLF 2D, developed at the University of Liege and based on a finite volume scheme.

Mathematical Model

The hydraulic model is based on the two-dimensional depth-averaged equations of volume and momentum conservation, namely the "shallow-water" equations (SWE). In the "shallow-water" approach the basic assumption states that velocities normal to a main flow direction are smaller than those in this main flow direction. As a consequence the pressure field is found to be almost hydrostatic everywhere.

The large majority of flows occurring in rivers, even highly transient, can reasonably be seen as shallow everywhere, except in the vicinity of some singularities (e.g. weirs). Indeed, vertical velocity components remain generally low compared to velocity components in the horizontal plane and, consequently, flows may be considered as mainly two-dimensional. Therefore, the approach presented here may definitely be regarded as suitable for floodplain inundation modelling.

Conservation Laws

The conservative form of the depth-averaged equations of volume and momentum conservation can be written as follows, using vector notations,

$$\frac{\partial \mathbf{s}}{\partial t} + \frac{\partial \mathbf{f}}{\partial x} + \frac{\partial \mathbf{g}}{\partial y} + \frac{\partial \mathbf{f}_{\mathrm{d}}}{\partial x} + \frac{\partial \mathbf{g}_{\mathrm{d}}}{\partial y} = \mathbf{S}_0 - \mathbf{S}_{\mathrm{f}}, \tag{1}$$

with $\mathbf{s} = [h\ hu\ hv]^{\mathrm{T}}$ the vector of the conservative unknowns. $\mathbf{f}$ and $\mathbf{g}$ represent the advective and pressure fluxes in directions x and y, while. $\mathbf{f}_{\mathrm{d}}$ and $\mathbf{g}_{\mathrm{d}}$ are the diffusive fluxes:

$$\mathbf{f} = \begin{pmatrix} hu \\ hu^2 + \frac{1}{2} gh^2 \\ huv \end{pmatrix}, \quad \mathbf{f}_{\mathrm{d}} = -\frac{h}{\rho}\begin{pmatrix} 0 \\ \sigma_x \\ \tau_{xy} \end{pmatrix}, \tag{2}$$

$$\mathbf{g} = \begin{pmatrix} hv \\ huv \\ hv^2 + \frac{1}{2} gh^2 \end{pmatrix}, \quad \mathbf{g}_{\mathrm{d}} = -\frac{h}{\rho}\begin{pmatrix} 0 \\ \tau_{xy} \\ \sigma_y \end{pmatrix}. \tag{3}$$

$\mathbf{S}_0$ and $\mathbf{S}_{\mathrm{f}}$ designates respectively the bottom slope term and the friction term:

$$\mathbf{S}_0 = -gh\left[0 \quad \partial z_{\mathrm{b}}/\partial x \quad \partial z_{\mathrm{b}}/\partial y\right]^{\mathrm{T}}, \tag{4}$$

$$\mathbf{S}_{\mathrm{f}} = \left[0 \quad \tau_{\mathrm{b}x}/\rho \quad \tau_{\mathrm{b}y}/\rho\right]^{\mathrm{T}}. \tag{5}$$

The following notations have been used: t = time; x and y = space coordinates; h = water depth, u and v = depth-averaged velocity components, z_{b} =bottom elevation, g = gravity acceleration, ρ = density of water, τ_{bx} and τ_{by} = bottom shear stresses, σ_x and σ_y = turbulent normal stresses, and τ_{xy} = turbulent shear stress.

Closure Relations: Friction and Turbulence

The bottom friction is conventionally modelled thanks to an empirical law, such as the Manning formula. The model enables the definition of a spatially distributed roughness coefficient. Besides, the friction along side walls is reproduced by means of a process-oriented formulation (Dewals *et al.* 2008a; Dewals *et al.* 2008d):

$$\frac{\tau_{\mathrm{b}x}}{\rho g h} = u\left[\sqrt{u^2 + v^2}\,\frac{n_{\mathrm{b}}^2}{h^{4/3}} + \sum_{k_x=1}^{N_x} \frac{4}{3}\,\frac{u\ n_{\mathrm{w}}^2}{h^{1/3}\Delta y}\right], \tag{6}$$

$$\frac{\tau_{\mathrm{b}y}}{\rho g h} = v\left[\sqrt{u^2 + v^2}\,\frac{n_{\mathrm{b}}^2}{h^{4/3}} + \sum_{k_y=1}^{N_y} \frac{4}{3}\,\frac{v\ n_{\mathrm{w}}^{3/2}}{h^{1/3}\Delta x}\right], \tag{7}$$

where the Manning coefficients n_{b} and n_{w} (s/m$^{1/3}$) characterize respectively the bottom and the side-walls roughness. Those relations are particularized for Cartesian grids, as exploited in the present study.

The internal friction may be accounted for thanks to the turbulence model included in WOLF 2D. The turbulent stresses are expressed following the Boussinesq approximation (Rodi 1984; ASCE Task Committee on Turbulence Models in Hydraulic Computations 1988):

$$\frac{\sigma_x}{\rho} = 2\left(\nu + \nu_{\mathrm{T}}\right)\frac{\partial u}{\partial x}, \quad \frac{\sigma_y}{\rho} = 2\left(\nu + \nu_{\mathrm{T}}\right)\frac{\partial v}{\partial y}, \tag{8}$$

$$\frac{\tau_{xy}}{\rho} = \frac{\tau_{yx}}{\rho} = \left(\nu + \nu_{\mathrm{T}}\right)\left(\frac{\partial u}{\partial y} + \frac{\partial v}{\partial x}\right), \tag{9}$$

where ν = molecular kinematic viscosity, ν_{T} = eddy viscosity computed by a turbulence closure model (ν † ν_{T}). For this purpose, two different approaches are available in WOLF 2D:

- first, a simple algebraic turbulence closure, assuming that the turbulence is bed-dominated, leading to the following expression for the turbulent kinematic viscosity: $\nu_{\mathrm{T}} = \alpha h u_*$, with α taking values of the order 0.5 (Fischer *et al.* 1979);
- second, an original depth-averaged k-ε model with two length-scales accounting

for vertical and horizontal turbulence mixing, as developed by Erpicum (2009b).

Computational Implementation

Space Discretization

The computation domain is discretized by means of a multiblock grid, in which each block consists in a locally Cartesian mesh. Since this multiblock structure enables refined meshes close to interesting areas, it compensates for the usual drawbacks of Cartesian grids, while keeping the benefits of structured grids in terms of accuracy and computation time.

The space discretization of the divergence form of the 2D conservative shallow-water equations is performed by means of a finite volume scheme. Within each block, variable reconstruction at cells interfaces can be performed by constant or linear extrapolation, in conjunction with a slope limiter, leading respectively to a first or second order accuracy. Variables at the border between adjacent blocks are extrapolated linearly, using additional ghost points. The value of the variables at the ghost points is evaluated from the value of the subjacent cells. Moreover, to ensure conservation properties at the border between adjacent blocks and thus to compute accurate volume and momentum balances, fluxes related to the larger cells are computed at the level of the finer ones.

Appropriate flux computation has always been a challenging issue in computational fluid dynamics. In the present study, fluxes **f** and **g** are computed by a Flux Vector Splitting (FVS) method developed by the authors. According to this FVS, the upwinding direction of each term of the fluxes **f** and **g** is simply dictated by the sign of the flow velocity reconstructed at the cells interfaces. It has thus the advantage of being completely Froude independent and of facilitating a satisfactory adequacy with the discretization of the bed elevation gradient (Erpicum *et al.* 2009a). A Von Neumann stability analysis has demonstrated that this FVS leads to a stable spatial discretization of the terms $\partial \mathbf{f}/\partial x$ and $\partial \mathbf{g}/\partial y$ in Equation 1.

This FVS has already proved its validity and efficiency for numerous applications (Dewals *et al.* 2006a; Dewals *et al.* 2008d; Erpicum *et al.* 2009b), including inundation mapping (Archambeau *et al.* 2004; Dewals *et al.* 2008a; Erpicum *et al.* 2008) and dam break flow simulations (Dewals *et al.* 2006b; Erpicum *et al.* 2009a; Roger *et al.* 2009). Due to their diffusive nature, the fluxes $\mathbf{f}_d$ and $\mathbf{g}_d$ are legitimately evaluated by means of a centred scheme.

Time Discretization

Since the model is applied to compute steady-state solutions, the time integration is performed by means of a three-step first order accurate Runge-Kutta algorithm, providing adequate dissipation in time. For stability reasons, the time step is constrained by the Courant–Friedrichs–Levy (CFL) condition. A semi-implicit treatment of the bottom friction term (3) is used, without requiring additional computational costs.

Boundary Conditions

The value of the specific discharge is prescribed as an inflow boundary condition. Besides, the transverse specific discharge is set to zero at the inflow. The outflow boundary condition may be a prescribed water surface elevation, a Froude number or no condition in case of supercritical outflow. At solid walls, the component of the specific discharge normal to the wall is set to zero. For the purpose of evaluating the diffusive terms, the gradients of the unknowns must also be specified at the boundaries. These gradients in the direction parallel to the boundary are set to zero, while the gradients of the variables in the direction normal to the boundary are evaluated by finite difference between the boundary and the centre of the next cell (Erpicum *et al.* 2009b).

Mesh Adaptation and Automatic Refinement

A grid adaptation technique is used to restrict the computation domain to the wet cells and a narrow strip surrounding these wet cells. The grid is thus adapted at each time step. As a result of an iterative resolution of the continuity equation prior to the evaluation of the momentum equations, wetting and drying of computation cells is handled free of volume and momentum conservation errors, as reported by Dewals *et al.* (2008a) and also used by Roger *et al.* (2009).

In addition, the model includes an *automatic mesh refinement* algorithm (AMR). For steady-state simulations, the AMR tool consists in performing the computation on several successive grids, starting from a coarse one and gradually refining it up to the finest one (Archambeau *et al.* 2004; Dewals *et al.* 2008a). When the hydrodynamic fields are stabilized on one grid, the solver automatically jumps onto a finer one. The successive solutions are interpolated from the coarser towards the finer grid. This fully automatic method considerably reduces the number of cells in the first grids, while increasing the time step, and thus substantially reduces the total run time, despite slight extra computation time required for meshing and interpolation operations.

Other Features

The herein described model constitutes a part of the modelling system “WOLF”, developed at the University of Liege. WOLF includes a set of complementary and interconnected modules for simulating free surface flows: process-oriented hydrology (Khuat Duy *et al.* 2009), 1D & 2D hydrodynamics, sediment (Dewals *et al.* 2008b) or pollutant transport, air entrainment, as well as an optimisation tool based on Genetic Algorithms.

Other functionalities of WOLF 2D include the use of moment of momentum equations, the application of the cut-cell method, as well as computations considering bottom curvature effects by means of curvilinear coordinates in the vertical plane (Dewals *et al.* 2006a).

A user-friendly interface, entirely designed and implemented by the authors, makes the pre- and post-processing operations particularly convenient. Import and export operations are easily feasible from and to various classical GIS tools. Several layers can be handled to make the analysis of various data sets easier such as topography, land use, vegetation density, hydrodynamic fields...

Application to Inundation Mapping

Topographic Data and Inundation Mapping

For about a decade, high resolution high accuracy topographic datasets have become increasingly available for inundation modelling in a number of countries. In Belgium, a data collection programme using airborne laser altimetry (Light Detection And Ranging - LiDAR) has generated high quality topographic data covering the floodplains of most rivers in the southern part of the country. Simultaneously, the bathymetry of the main rivers has been surveyed by means of an echo-sonar technique.

Consequently, combining data generated from those two remote sensing techniques enables to obtain a complete Digital Surface Model (DSM) characterized by a horizontal resolution of 1 m by 1 m and with a vertical accuracy of 15 cm. As regards non navigable rivers, cross sections are properly interpolated in order to generate a two-dimensional bathymetry.

Those high quality topographic data combined with simulations performed on grids as fine as 2 m by 2 m enable to set the value of roughness coefficients to represent only small scale roughness elements and not to globalize larger scale effects such as blockage by buildings or by large irregularities of the topography. It also enables to conduct inundation modelling at the scale of each house and street individually.

Nevertheless, since inundation flows may be extremely sensitive to some local topographic characteristics, such as for instance the exact height of a protection wall, a crucial step consists in validating and enhancing the DSM by removing automatically residual obstacles non relevant for the flow such as vegetation. Another important pre-processing step is the integration of additional sources of topographic data (including field survey) as well as the detailed geometry of flood protections and other hydraulic structures (weirs, water intakes …). The large amount of data collected from those various sources is stored within an efficient database structure.

Steady State Approach

All numerical simulations detailed in the present chapter refer to river reaches located in the sub-basin of river Meuse situated in Belgium. As detailed by de Wit et al. (2007), in the central part of the Meuse basin, between Charleville-Mézières and Liège, rivers are captured in the Ardennes massif, characterized by narrow steep valleys, where flood waves are hardly attenuated.

Consequently, flood waves along this type of rivers are hardly attenuated as a result of the combination of the steep longitudinal gradients and of the relatively narrow cross-sectional shape of the valleys (de Wit *et al.* 2007), leading to relatively low storage capacity in the floodplains. As a result the floodplains are completely filled with water quickly after the beginning of the flood and a quasi-steady flow is then observed.

For instance, for typical floods occurring on river Ourthe, it has been verified that the volume of water stored in the inundated floodplains along a 10 km-long reach remains lower than one percent of the total amount of water brought by the flood wave.

Besides, comparisons have been made between inundation patterns predicted by unsteady flow simulations, for which the real flood hydrograph is prescribed as an upstream boundary condition, and inundation patterns computed assuming a steady-state flow (constant discharge close to the peak discharge of the hydrograph). Those comparisons have confirmed that the maximum flood extents predicted by the two approaches are in very good agreement.

Therefore, the steady-state assumption has been considered as valid for simulating floodplain inundation along most rivers of the Ardennes Massif and is systematically used in the simulations discussed in the subsequent paragraphs. An additional benefit of this assumption is reduced run time as a result of the possibility to exploit automatic mesh refinement.

Free surface elevation is prescribed as a boundary condition, based either on the simulation result of a downstream reach or on a stage-discharge curve at a gauging station. Since relatively short reaches are considered, without main tributaries, the lateral inflows are neglected.

Model Validation

The two-dimensional flow model used for inundation modelling WOLF 2D has been comprehensively validated. First, the accuracy of the modelling system has been established based on a number of standard benchmarks. Secondly, results of inundation mapping have been compared with observations from historical flood events. Data collected during these events have been used to confirm the validity of the flow model for inundation mapping.

Gauging Stations

First, the water depth (or free surface elevation) computed by WOLF 2D has been compared to observed water levels at gauging stations. Figure 7 shows observed water levels at two gauging stations (plotted in grey), while the black curves represent computed water levels for six simulated discharges. The later match fairly well the observations. The gauging stations are respectively located on river Vesdre (Figure 7 a.), which is a tributary of river Ourthe, and on river Semois (Figure 7 b.), a tributary of river Meuse. The maximum modelled discharges are respectively 300 m³/s for river Vesdre and 750 m³/s for river Semois.

In the same scope, Figure 8 and Table 1 compare water elevations measured during the December 1993 flood on river Amblève, another tributary of river Ourthe, with the numerical computation of the same event. Table 1 confirms the satisfactory agreement between the results of hydraulic modelling and the observations of the real event. The difference remains systematically lower than 4 centimetres.

Aerial Imagery

Another way to validate the hydraulic model consists in comparing simulated flood extent with aerial pictures, taken at the time of the peak discharge. Figure 9 illustrates the results of this validation at Wanlin, on river Lesse during the January 1995 flood (discharge = 180 m³/s – corresponding to a 15-year return period). The numerical results (Figure 9 b.) represent the flood extension, which is in good agreement with the picture of the real event (Figure 9 a.). The caravans in the campsite have been removed from the DSM since they don't constitute obstacles relevant for the flow. Indeed, in this kind of residential campsite most caravans are built on piles (Figure 9 – Point 2).

Figure 7. Validation of the hydraulic model WOLF based on gauging station measurements

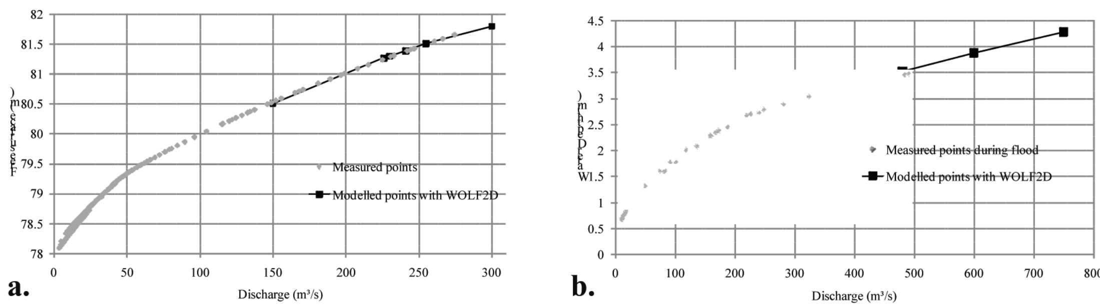

Figure 8. Computed inundation extent for the December 1993 flood on a 3 km long reach of river Amblève (peak discharge = 298 m³/s) and location of the 4 points mentioned in Table 1

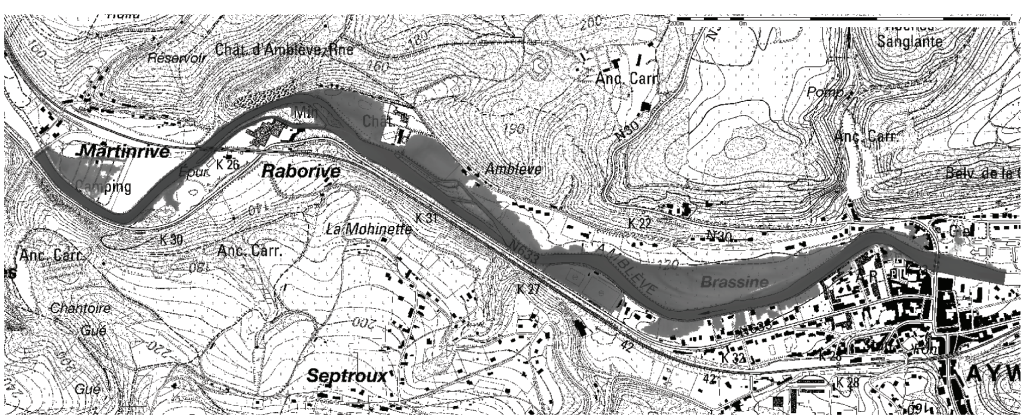

Table 1. Comparison between water elevations survey and numerical results on river Amblève

Location	*Real event [m]*	*Numerical results [m]*
Pt. 1: Martinrive bridge (boundary condition)	**112.77**	**112.77**
Pt. 2: Downstream of the football field	**118.38**	**118.4**
Pt. 3: Aywaille boarding school	**119.81**	**119.85**
Pt. 4: Bridge of Aywaille	**120.81**	**120.85**

APPLICATION: ASSESSMENT OF PROTECTION MEASURES

Case Study Description

The considered case study is located in the lower part of river Ourthe (Belgium), the catchment of which has an area of about 2900 km^2 at the downstream limit of the case study. The risk analysis has been applied to three reaches of the river, situated respectively 18.5 km (reach n°1), 12.5 km (reach n°2) and 10 km (reach n°3) upstream of the mouth of river Ourthe into river Meuse. The total length of the simulated reaches is about 16 km, with a computational Cartesian grid of 2 by 2 meters, leading to a total number of 8.2 × 10^5 computational cells. Two municipalities are situated along the studied part of river Ourthe: Esneux and Tilff.

Over the last 25 years, communities living along the river have experienced four major flood events: (1) in 1993 flooding occurred with a maximum peak discharge of 742 m³/s; (2) in 1995, 520 m³/s; (3) in 2002, 570 m³/s; (4) in 2003, 508 m³/s. During these floods validation data were collected, such as aerial pictures and gauging station measurements. With the aim of validating the hydraulic modelling for the studied area, these historic flood events have been simulated and results were found to compare reasonably well with observations.

Concerning hydraulic modelling, the case study is located in the Ardennes massif, where the valleys are relatively narrow and the storage capacity in the floodplains remains very low. As discussed above, the steady state assumption is thus valid for inundation modelling.

Available GIS Data

A micro-scale risk analysis has to handle large sets of geographic information, such as land use data, with different spatial resolution and quality. The main GIS data available in the area of the case study are listed and described below.

Figure 9. Flood event on river Lesse (January 1995, discharge = 180 m³/s); (a) aerial picture, (b) modelled inundation extent

Land Use Databases

In Belgium, there are several geographic land use data producers, the most important of which are: the Belgian *Institut Géographique National* - IGN and the *Service Publique de Wallonie* - SPW. Both provide accurate land use vector database, respectively named Top10v-GIS and PICC. The first one contains 18 layers related to information categories (e.g. land use, structure, hydrography...), while the PICC data set is based on stereoscopic aerial imagery restitution and a post processing enrichment with ancient database such as house number, street name…

Both PICC and Top10v-GIS data constitute detailed and accurate complementary spatial database at a very high scale (1:10000). The challenge is to extract the strong points from each database and to combine them into a single data set in order to identify with maximal accuracy the elements-at-risk (geometric aspect) and their type or use (semantic aspect).

Land Registry

The Land Registry lists all private properties and an index related to their value. The information is also recorded in a geographic database, i.e. each asset listed in this database is located. But since this register is partly based on older data sources, its geometric accuracy is significantly lower compared to the others databases. Thus, the geometric information from the Land Registry is not exploited here, but only its semantic content is used with the single purpose of estimating the economic value of the goods.

Statistical Data

Belgium is subdivided into a large number of statistical sectors, for which statistical data are available, such as number of inhabitants, average age, … These data are used in the social study (Coninx & Bachus 2007) providing estimates for the social vulnerability of people and adaptive capacity of society.

Summary

The challenge of a micro-scale analysis is to deal with several sources of complementary GIS data sets characterized by different geometric and semantic levels of quality. With the aim of summarizing this section, Table 2 lists available data and characterizes their quality and main features.

Situation without New Flood Protection Measure

Before evaluating the impact of possible protection measures, it is important to assess the risk in the current situation without additional flood protections. In this framework, fourteen return periods have been considered, leading to inunda-

Table 2. Geometric and semantic characteristics of relevant geographic data sets

Data	*Format*	*Geometric quality*	*Semantic quality*	*Features used in the risk analysis*	*Availability*
LiDAR	**Raster**	+	-	**Accurate elevation (DSM)**	**Floodplain of main river**
Top10v-GIS	**Vector**	+	+	**Very rich land use data**	**Everywhere**
PICC	**Vector**	+	+	**Eg. cornice height, single buildings**	**Not in rural area**
Land registry	**Vector**	-/+	+	**Mainly economic information**	**Privacy conditions**
Statistical data	**Vector**	-	+	**Mainly socio-economic data**	**Everywhere**

tion modelling for fourteen different discharge values (Table 3):

- four historical flood events (1993, 1995, 2002 and 2003) used to validate the hydraulic model;
- discharges corresponding to two statistical return periods, namely 25- and 100-year;
- eight additional discharges (statistical return period increased by 5, 10, 15 and 30 percent).

Hydraulic simulations have been performed with the flow model WOLF 2D described detail above. The validation of the model was achieved by comparison of computed and observed inundation extent for four historical flood events. As shown above, the inundation extent predicted by numerical modelling agrees with the observed one.

The main outputs of the risk analysis procedure are provided in Figures 5 and 6. Another significant result, obtained thanks to the semantic quality of the GIS available in the studied area,

Table 3. Considered return periods and corresponding discharges

		1993	***1995***	***2002***	***2003***
Discharge [m³/s]		742	520	570	508
	25-year	25+5%	25+10%	25+15%	25+30%
Discharge [m³/s]	726	762.3	798.6	834.9	943.8
	100-year	100+5%	100+10%	100+15%	100+30%
Discharge [m³/s]	876	919.8	963.6	1007.4	1138.8

Table 4. Example of inventory of affected buildings, automatically obtained from the exposure analysis (■ water depth ≥ 1.3m, ▣ 1.3m ≥ water depth > 0.3m, □ water depth ≤ 0.3m)

Return period [year]	**4**	**5**	**7**	**25**	**29**	**34**	**48**	**68**	**100**	**154**	**100+5%**	**100+10%**	**100+15%**	**100+30%**
Hospital	□	□	□	▣	▣	▣	▣	▣	▣	▣	▣	▣	▣	▣
Camping Site	▣	▣	▣	▣	▣	▣	■	■	■	■	■	■	■	■
Supermarket			□	□	□	□	□	□	□	▣	▣	▣	▣	▣
Church				□	□	□	□	▣	▣	▣	▣	▣	▣	▣
School					□	□	□	□	□	▣	▣	▣	▣	▣
Petrol station							□	□	□	▣	▣	▣	▣	▣
Petrol station									□	□	□	□	□	▣
Recreational facility											□	□	□	▣
Castel												□	▣	▣
SME													□	▣
Engineering company													□	▣
Supermarket													□	▣
Factory														□

is the identification of all affected buildings and facilities, as shown in Table 4. In this table, the grey scale indicates the computed water level inside the inundated assets.

Flood Protection Measure: Mobile Dikes

The flood protection measure studied for the application of the risk evaluation methodology is the heightening of an existing protection wall by means of mobile dikes. The existing protection wall was originally designed to protect the town of Esneux from a 20-year flood. The mobile dikes would enable to extend the range of discharges and thus return periods for which protection remains effective.

This measure has a number of interesting advantages such as the little visual inconvenience for local communities and limited investment costs. In contrast, emergency teams need to remain ready and operational in the case of flood warnings.

Figure 10 shows an aerial picture of the town Esneux during the 1995-flood. The picture was taken approximately at the peak discharge of 520m^3/s. The black lines drawn along the riverside indicate the projected location for additional mobile dikes. The following analysis focuses on the residential area located on the left bank of the river.

Risk Analysis

The methodology of risk evaluation has been applied for the case study. The first output of the methodology is the result of the social impact evaluation, expressed by the number of people affected by low, medium or high social impacts.

Figure 11 reveals that no inhabitants of the floodplain are highly socially vulnerable with respect to flood. It also appears that, for river discharges lower than approximately 900 m^3/s, the mobile dike has a beneficial effect, while it causes more people to be affected by flood for discharges exceeding 900 m^3/s. This result is due to the reduction of the cross-section of the river when mobile dikes are implemented, leading to higher water heads in the upstream part of the river reach. This is confirmed in Figure 12, which shows the evolution of the water level as a function of the discharge for two representative points in the main channel (point A and B in Figure 10), located respectively upstream and downstream of the mobile dikes.

Figure 13 shows the estimated direct tangible damage to housing for the whole range of con-

Figure 10. Aerial picture of the town of Esneux during the 1995 flood event (peak discharge 520 m^3/s)

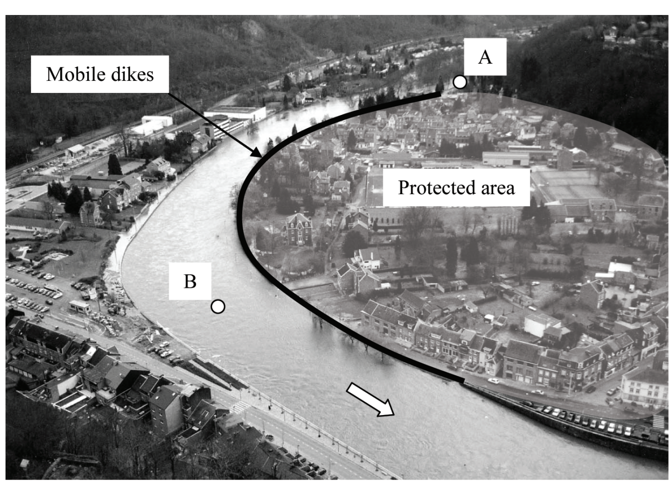

Figure 11. Number of people threatened by flooding as a function of the discharge (grey curves: number of people with low social vulnerability, black curves: total number of people with low to medium social vulnerability)

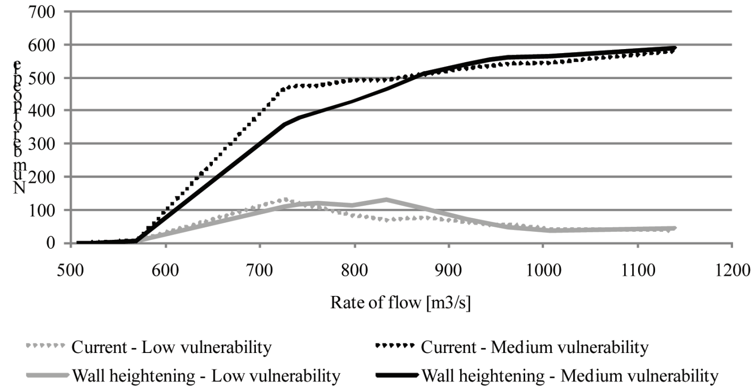

Figure 12. Computed water depth as a function of the discharge at two representative locations in the main channel (see Figure 10)

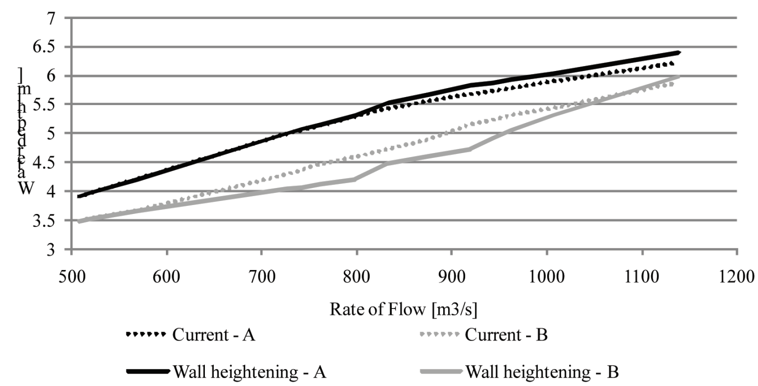

Figure 13. Estimated direct tangible monetary losses to housing with (continuous curve) and without the mobile dikes (dotted curve)

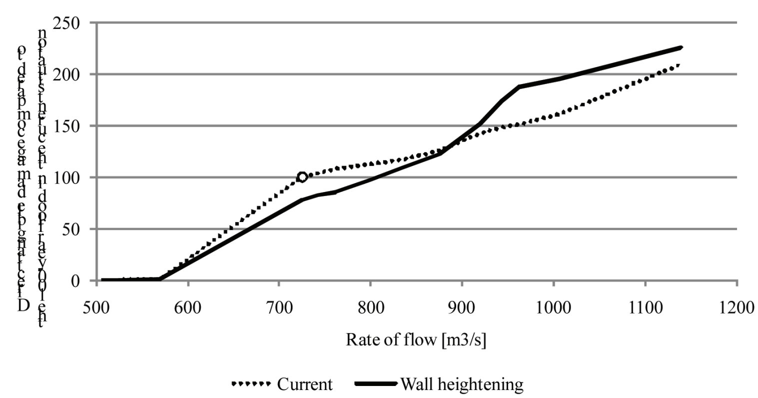

sidered flood events, from low discharge inducing hardly any losses to extreme events. Monetary damage is expressed as a percentage of the damage induced in the case of the 100-year flood in the present situation. Once again, mobile dikes reduce damage for discharges below 900 m³/s, whereas for higher discharges the increased water level upstream of the mobile dikes causes higher economic damage than in the present situation.

This definitely confirms the practical need to evaluate projected flood protection measures based on the analysis of flow for a relatively wide range of discharges (and thus return periods) and not to base the assessment on just a single "design discharge" or "design return period".

CONCLUSION

A consistent micro-scale flood risk modelling methodology has been presented, which leads to practical outcomes for assessing flood management strategies and handles detailed hydraulic modelling in 2D (including velocity fields in the floodplain). The methodology succeeds in automatically evaluating the exposure and the socio-economic flood risk for a wide range of discharges on large flood-prone areas. High resolution object-oriented geographic databases are effectively handled by the procedure, thus drastically reducing the need for field surveys. In conclusion, the present paper describes an innovative, reliable and practical tool, which may be used both for assessing the impact of climate change on flood risk and for evaluating adaptation strategies.

REFERENCES

Apel, H., Aronica, G., Kreibich, H., & Thieken, A. (2007). Flood Risk Assessment strategies? a comparative study. *Geophysical Research Abstracts*, *9*(02916).

Archambeau, P., Dewals, B., Detrembleur, S., Erpicum, S., & Pirotton, M. (2004). A set of efficient numerical tools for floodplain modeling. In G. H. Jirka and W. S. J. Uijttewaal. Leiden, (eds.), *Shallow Flows.* Balkema**:** 549-557.

ASCE Task Committee on Turbulence Models in Hydraulic Computations. (1988). Turbulence modeling of surface water flow and transport: Part I. *Journal of Hydraulic Engineering*, *114*(9), 970–991. doi:10.1061/(ASCE)0733-9429(1988)114:9(970)

Coninx, I., & Bachus, K. (2007). *Integrating social vulnerability to floods in a climate change context*. In *Proc. Int. Conf. on adaptive and integrated water management, coping with complexity and uncertainty*, Basel, Switzerland.

de Wit, M. J. M., Peeters, H. A., Gastaud, P. H., Dewil, P., Maeghe, K., & Baumgart, J. (2007). Floods in the Meuse basin: event descriptions and an international view on ongoing measures. *Intl. J. River Basin Management*, *5*(4), 279–292.

Dewals, B. J., Detrembleur, S., Archambeau, P., Erpicum, S., & Pirotton, M. (2008a). Detailed 2D hydrodynamic simulations as an onset for evaluating socio-economic impacts of floods considering climate change. In Samuels, P., Huntington, S., Allsop, W., & Harrop, J. (Eds.), *Flood Risk Management: Research and Practice*. London: Taylor & Francis.

Dewals, B. J., & Erpicum, S. Archambeau, P. Detrembleur, S., & Pirotton, M. (2006b). Numerical tools for dam break risk assessment: validation and application to a large complex of dams. *Improvements in reservoir construction, operation and maintenance*. H. Henry. London, Thomas Telford (pp. 272-282).

Dewals, B. J., Erpicum, S., Archambeau, P., Detrembleur, S., & Pirotton, M. (2006a). Depth-integrated flow modelling taking into account bottom curvature. *Journal of Hydraulic Research*, *44*(6), 787–795.

Dewals, B. J., Erpicum, S., Archambeau, P., Detrembleur, S., & Pirotton, M. (2008b). "Hétérogénéité des échelles spatio-temporelles d'écoulements hydrosédimentaires et modélisation numérique." *Houille Blanche-Rev. Int.* (5), 109-114.

Dewals, B. J., Giron, E., Ernst, J., Hecq, W., & Pirotton, M. (2008c). Integrated assessment of flood protection measures in the context of climate change: hydraulic modelling and economic approach. In Aravossis, K. (Eds.), *Environmental Economics*.

Dewals, B. J., Kantoush, S. A., Erpicum, S., Pirotton, M., & Schleiss, A. J. (2008d). Experimental and numerical analysis of flow instabilities in rectangular shallow basins. *Environmental Fluid Mechanics*, *8*, 31–54. doi:10.1007/s10652-008-9053-z

Ernst, J., Coninx, I., Dewals, B. J., Detrembleur, S., Erpicum, S., Bachus, K., & Pirotton, M. (2009a). Social Flood Impacts in Urban Areas: Integration of Detailed Flow Modelling and Social Analysis. In *Proc. 33rd IAHR Congress - Water engineering for a sustainable environment*. Vancouver, British Columbia: IAHR.

Ernst, J., Coninx, I., Dewals, B. J., Detrembleur, S., Erpicum, S., Pirotton, M., & Bachus, K. (2009b). Planning flood risk reducing measures based on combined hydraulic simulations and socio-economic modelling at a micro-scale. In *Proceedings of the European Water Ressources Association 7th Int. Conf. - Water Resources Conservation and Risk Reduction Under Climatic Instability*. Limassol, Cyprus.

Ernst, J., & Dewals, B. J. Detrembleur, S. Archambeau, P. Erpicum, S., & Pirotton, M. (2008). Integration of accurate 2D inundation modelling, vector land use database and economic damage evaluation. P. Samuels, S. Huntington, W. Allsop and J. Harrop. London, Taylor & Francis (eds.), *Flood Risk Management: Research and Practice*. (pp. 1643-1653).

Erpicum, S., Archambeau, P., Detrembleur, S., Dewals, B., & Pirotton, M. (2008). *A 2D finite volume multiblock flow solver applied to flood extension forecasting. Numerical modelling of hydrodynamics for water ressources. G.-N. Pilar and P. Enrique*. London: Taylor & Francis.

Erpicum, S., Meile, T., Dewals, B. J., Pirotton, M., & Schleiss, A. J. (2009a). Dam-break flow computation based on an efficient flux-vector splitting. *J. Comput. Appl. Math.*

Erpicum, S., Meile, T., Dewals, B. J., Pirotton, M., & Schleiss, A. J. (2009b). 2D numerical flow modeling in a macro-rough channel. *Int. J. Numer. Methods Fluids*.

EU. *(2007)*. Directive 2007/60/EC of the European Parliament and of the Council on the assessment and management of flood risks. *Strasbourg*.

Fischer, H. B., List, E. J., Koh, R. C. Y., Imberger, J., & Brooks, N. H. (1979). *Velocity Distribution in Turbulent Shear Flow. Mixing in Inland and Coastal Waters*. New York: Academic Press.

IPCC(2001). Climate Change 2001: Impacts, Adaptation and Vulnerability, Intergovernmental Panel on Climate Change, *1032*.

Kaplan, S., & Garrick, B. J. (1981). On The Quantitative Definition of Risk. *Risk Analysis*, *1*, 11–27. doi:10.1111/j.1539-6924.1981.tb01350.x

Khuat Duy, B., Archambeau, P., Dewals, B. J., Erpicum, S., & Pirotton, M. (2009). *Mitigating flood impacts in a Belgian catchment*. Proc. Inst. Civil. Eng.-Water Manag.

McMillan, H. K., & Brasington, J. (2008). End-to-end risk assessment: A coupled model cascade with uncertainty estimation. *Water Resources Research*, *44*(W03419), 14. doi:10.1029/2007WR005995

Merz, B. (2006). *Hochwasserrisiken: Grenzen und Möglichkeiten der Risikoabschätzung*. Stuttgart: Schweizerbart'sche Verlagsbuchhandlung.

Merz, B., Kreibich, H., Thieken, A., & Schmidtke, R. (2004). Estimation uncertainty of direct monetary flood damage to buildings. *Natural Hazards and Earth System Sciences*, *4*(1), 153–163. doi:10.5194/nhess-4-153-2004

Rodi, W. (1984). *Turbulence models and their application in hydraulics - A state-of-the-art*. Rotterdam, UK: Balkema.

Roger, S., Dewals, B. J., Erpicum, S., Schwanenberg, D., Schüttrumpf, H., Köngeter, J., & Pirotton, M. (2009). Experimental und numerical investigations of dike-break induced flows. *Journal of Hydraulic Research*, *47*(3), 349–359. doi:10.3826/jhr.2009.3472

Smith, D. I. (1994). Flood damage estimation - A review of urban stage damage curves and loss function. *Water S.A.*, *20*(3), 231–238.

Thieken, A., Ackermann, V., Elmer, F., Kreibich, H., Kuhlmann, B., Kunert, U., et al. (2008). Methods for the evaluation of direct and indirect flood losses. In *Proc. 4th Int. Symp. on Flood Defence*. Toronto, Canada: Institue for Catastrophic Loss Reduction.